Chaotic Scattering on Graphs

Tsampikos Kottos[1] and Uzy Smilansky[2]

[1]*Max-Planck-Institut für Strömungsforschung, 37073 Göttingen, Germany*
[2]*Department of Physics of Complex Systems, The Weizmann Institute of Science, 76100 Rehovot, Israel*

Quantized, compact graphs are excellent paradigms for quantum chaos in bounded systems. Connecting them with leads to infinity, we show that they display all the features which characterize quantum chaotic scattering. We derive exact expressions for the scattering matrix, and an exact trace formula for the density of resonances, in terms of classical orbits, analogous to the semiclassical theory of chaotic scattering. A statistical analysis of the cross sections and resonance parameters compares well with the predictions of random matrix theory. Hence, this system is proposed as a convenient tool to study the generic behavior of chaotic scattering systems and their semiclassical description.

PACS numbers: 05.45.Mt, 03.65.Sq

Quantum graphs provide a very useful tool to study bounded quantum systems which are chaotic in the classical limit [1]. Here, by attaching infinite leads we turn the compact graphs into scattering systems, and show that they display chaotic scattering [2,3], a phenomenon with applications in many fields, ranging from nuclear [4], atomic [5], and molecular [3] physics to mesoscopics [6] and classical wave scattering [7]. We express the *quantum* scattering matrix and the trace formula for the density of its resonances in terms of the orbits of the underlying *classical* scattering system. These expressions are the exact analogs of the corresponding semiclassical approximations available in the theory of chaotic scattering [2,8,9]. With these tools we analyze the distribution of resonances and the statistics of the fluctuating scattering amplitudes and cross sections. We show that graphs provide new insight on the connection between random matrix theory (RMT) and chaotic scattering. Moreover, we illustrate their advantages as versatile and convenient tools for numerical studies of chaotic scattering.

Consider first a *bounded* graph $\mathcal{G}$. It consists of V *vertices* connected by *bonds*. The valency v_i of a vertex i is the number of bonds which emanate from it, and we allow only a single bond between any two vertices. The total number of bonds is $B = \frac{1}{2}\sum_{i=1}^{V} v_i$. The bond connecting the vertices i and j is denoted by $b \equiv (i, j)$. We shall also distinguish between the directions on the bond using $\hat{b} \equiv (j, i)$ to denote the reverse direction. The length of the bonds is denoted by L_b and we shall henceforth assume that they are *rationally independent*. In the *directed-bond* notation $L_b = L_{\hat{b}}$. The *scattering* graph $\tilde{\mathcal{G}}$ is obtained by adding infinite leads at the vertices of $\mathcal{G}$, changing their valency to $\tilde{v}_i = v_i + 1$. The leads are distinguished by the index i of the vertex to which they are attached.

The Schrödinger operator on the graph consists of the one-dimensional Laplacian $(-id_x - A_b)^2$ supplemented by boundary conditions on the vertices [1]. The "vector potentials" $A_b = -A_{\hat{b}}$ are introduced to break time reversal symmetry, and their value may vary from bond to bond.

On each of the bonds b or leads i, the wave function is expressed in terms of counterpropagating waves with a wave number k:

On the bonds: $\psi_b = a_b e^{i(k+A_b)x_b} + a_{\hat{b}} e^{i(k+A_{\hat{b}})(L_b - x_b)}$

On the leads: $\psi_i = I_i e^{-ikx_i} + O_i e^{ikx_i},$ (1)

where the coordinate x_b on the bond $b = (i, j)$ takes the value 0 (L_b) at the vertex i (j) while x_i measures the distance from the vertex along the lead i.

The amplitudes a_b, $a_{\hat{b}}$ on the bonds and I_i, O_i on the leads are determined by matching conditions at the vertices. They are expressed in terms of the $\tilde{v}_i \times \tilde{v}_i$ *vertex scattering matrices* $\Sigma_{j,j'}^{(i)}$, where j, j' go over all of the v_i bonds and the lead which emanate from i. The $\Sigma^{(i)}$ are symmetric *unitary* matrices, which guarantee current conservation at each vertex by requiring

$$\begin{pmatrix} O_i \\ a_{i,j_1} \\ \cdot \\ a_{i,j_{v_i}} \end{pmatrix} = \begin{pmatrix} \rho^{(i)} & \tau_{j_1}^{(i)} & \cdot & \tau_{j_{v_i}}^{(i)} \\ \tau_{j_1}^{(i)} & \tilde{\sigma}_{j_1,j_1}^{(i)} & \cdot & \tilde{\sigma}_{j_1,j_{v_i}}^{(i)} \\ \cdot & \cdot & \cdot & \cdot \\ \tau_{j_{v_i}}^{(i)} & \tilde{\sigma}_{j_{v_i},j_1}^{(i)} & \cdot & \tilde{\sigma}_{j_{v_i},j_{v_i}}^{(i)} \end{pmatrix} \begin{pmatrix} I_i \\ c_{j_1,i} \\ \cdot \\ c_{j_{v_i},i} \end{pmatrix},$$

    (2)

where $c_{j_l,i} = a_{j_l,i} e^{i(k+A_{(j_l,i)})L_{(i,j_l)}}$. Above, the vertex scattering matrix $\Sigma^{(i)}$ was written explicitly in terms of the vertex reflection amplitude $\rho^{(i)}$, the lead-bond transmission amplitudes $\{\tau_j^{(i)}\}$, and the $v_i \times v_i$ bond-bond transition matrix $\tilde{\sigma}_{j,j'}^{(i)}$, which is *subunitary* ($|\det\tilde{\sigma}^{(i)}| < 1$) due to the coupling to the leads. As an example, for v-regular graphs ($v_i = v \;\forall\; i$) with Neumann matching conditions on the vertices [1],

$$\tilde{\sigma}_{j,j'}^{(i)} = \frac{2}{v+1} - \delta_{j,j'};$$

$$\tau_j^{(i)} = \frac{2}{v+1}; \qquad \rho^{(i)} = \frac{2}{v+1} - 1. \qquad (3)$$

Combining Eqs. (2) for all of the vertices, we obtain the $V \times V$ scattering matrix $S^{(V)}$ which relates the outgoing and incoming amplitudes on the leads,

$$S_{i,j}^{(V)} = \delta_{i,j}\rho^{(i)} + \sum_{r,s} \tau_r^{(i)}[I - \tilde{S}(k;A)]_{(i,r),(s,j)}^{-1}D_{(s,j)}\tau_s^{(j)}.$$

(4)

Here, $D_{(s,j)}(k;A) = \exp[i(k + A_{(s,j)})L_{(s,j)}]$ is a diagonal matrix in the $2B$ space of directed bonds. The matrix $\tilde{S}(k;A) = D(k;A)\tilde{R}$ propagates the wave functions: $\tilde{R}$ assigns a scattering amplitude for transitions between connected directed bonds $\tilde{R}_{(i,r),(s,j)} = \delta_{r,s}\tilde{\sigma}_{i,j}^{(r)}$, $D(k;A)$ provides the phase due to free propagation. The matrix $\tilde{R}$ is subunitary, since $|\det\tilde{R}| = \prod_{i=1}^{V}|\det\tilde{\sigma}^{(i)}| < 1$. The scattering matrix (4) is interpreted in the following way. The prompt reflection at the entrance vertex induces a "direct" component. The "chaotic" component starts by a transmission from the incoming lead i to the bonds (i, r) with transmission amplitudes $\tau_r^{(i)}$. Multiple scattering is induced by $[I - \tilde{S}(k;A)]_r^{-1} = \sum_{n=0}^{\infty}\tilde{S}^n(k;A)$. The wave gains a phase $e^{i(k+A_b)L_b}$ for each bond it traverses, and a scattering amplitude $\tilde{\sigma}_{r,s}^{(i)}$ at each vertex, until it is transmitted from the bond (s, j) to the lead j with an amplitude $\tau_s^{(j)}$. Explicitly,

$$S_{i,j}^{(V)} = \delta_{i,j}\rho^{(i)} + \sum_{p\in\mathcal{P}_{i\to j}} \mathcal{B}_p e^{i(kl_p+b_p)},$$

(5)

where $\mathcal{P}_{i\to j}$ is the set of the trajectories on $\tilde{\mathcal{G}}$ which leads from i to j. $\mathcal{B}_p$ is the amplitude corresponding to a path p whose length and directed length are $l_p = \sum_{b\in p}L_b$ and $b_p = \sum_{b\in p}L_b A_b$, respectively. The scattering amplitude $S_{i,j}^{(V)}$ is a sum of a large number of partial amplitudes, whose complex interference brings about the typical irregular fluctuations of $|S_{i,j}^{(V)}|^2$ as a function of k.

The resonances are the (complex) zeros of

$$Z_{\tilde{\mathcal{G}}}(k) = \det[I - \tilde{S}(k;A)].$$

(6)

The eigenvalues of $\tilde{S}$ are in the unit circle, and therefore the resonances appear in the lower half of the complex k plane. Denoting the eigenvalues of $S^{(V)}(k)$ by $e^{i\theta_r(k)}$, $\det S^{(V)}(k) \equiv \exp[i\Theta(k)] = \exp[i\sum_{r=1}^{V}\theta_r(k)]$ is derived from (4) by standard manipulations [10], giving

$$\Theta(k) - \Theta(0) = -2\,\text{Im}\log\det[I - \tilde{S}(k;A)] + \mathcal{L}k.$$

(7)

$\mathcal{L} = 2\sum_{b=1}^{B}L_b$ is twice the total length of the bonds of $\tilde{\mathcal{G}}$. The resonance density $d_R(k)$ (which is proportional to the Wigner delay time) [2,11] is given by $d_R(k) \equiv \frac{1}{2\pi}\frac{d\Theta(k)}{dk}$. It assigns to each resonance a normalized Lorentzian centered at $\text{Re}(k_n)$ with a width $2\,\text{Im}(k_n)$. Hence,

$$d_R(k) = \frac{1}{2\pi}\mathcal{L} + \frac{1}{\pi}\text{Re}\sum_{n=1}^{\infty}\sum_{p\in\mathcal{P}_n} n_p l_p r\tilde{\mathcal{A}}_p^r e^{i(l_p k+b_p)r},$$

(8)

where the sum is over the set $\mathcal{P}_n$ of primitive periodic orbits whose period n_p is a divisor of n, with $r = n/n_p$. l_p and b_p are the length and the directed length, respectively,

and the amplitudes $\tilde{\mathcal{A}}_p$ are the products of the bond-bond scattering amplitudes $\tilde{\sigma}_{b,b'}$ along the primitive loops. The mean resonance spacing is given by $\Delta = 2\pi/\mathcal{L}$. Equation (8) is an exact trace formula for the resonance density.

The classical dynamics associated with $\tilde{\mathcal{G}}$ can be easily defined on the bonds, but not on the vertices which are singular points. However, a Liouville description is constructed (see [1]) by considering the evolution of a phase-space density over the $2B$ dimensional space of directed bonds. The corresponding evolution operator consists of the transition probabilities $\tilde{U}_{b,b'}$ between connected bonds b, b', taken from the corresponding quantum evolution operator $\tilde{U}_{b,b'} = |\tilde{R}_{b,b'}|^2$. Because of scattering to the leads $\sum_{b'}\tilde{U}_{bb'} < 1$, and the phase-space measure is not preserved but, rather, decays in time. Let $\tilde{p}_b(n)$ denote the probability to occupy the bond b at the (topological) time n. The probability to remain on $\tilde{\mathcal{G}}$ is

$$\tilde{P}(n) \equiv \sum_{b=1}^{2B}\tilde{p}_b(n) = \sum_{b,b'}\tilde{U}_{bb'}\tilde{p}_{b'}(n-1) \simeq e^{-\Gamma_{cl}n}\tilde{P}(0),$$

(9)

where $\exp(-\Gamma_{cl})$ is the largest eigenvalue of the "leaky" evolution operator $\tilde{U}_{bb'}$. For the v-regular graph (3), the probability to leak to the lead per time step is τ^2, hence, $\Gamma_{cl} \approx [2/(1 + v)]^2$. The set of trapped trajectories whose occupancy decays exponentially in time is the analog of the strange repeller in generic Hamiltonian systems displaying "chaotic scattering."

The formalism above can be easily modified for graphs where not all of the vertices are attached to leads. If l is not attached, one has to set $\rho^{(l)} = 1$, $\tau_j^{(l)} = 0$ in the definition of $\Sigma^{(l)}$. The dimension of $S^{(V)}$ is changed accordingly.

For generic graphs, the eigenvalues of the $\tilde{S}$ matrix are strictly inside the unit circle so the resonance widths $\Gamma_n \equiv -2\,\text{Im}(k_n)$ are excluded from the domain $\Gamma_n \geq \Gamma_{gap} = -2\log(|\lambda_{max}|)/L_{max}$, where λ_{max} is the largest eigenvalue of $\tilde{S}(0;A)$ and L_{max} is the longest bond. The existence of a gap—typical for chaotic scattering [3] from sufficiently open scatterers—is apparent in Fig. 1a. The widths are scaled by the mean spacing Δ between resonances, i.e., $\gamma_n \equiv \frac{\Gamma_n}{\Delta}$ so that $\langle\gamma\rangle_k$ determines whether the resonances are overlapping ($\langle\gamma\rangle_k > 1$) or isolated ($\langle\gamma\rangle_k < 1$) ($\langle\cdot\rangle_k$ denotes spectral averaging). The distribution of $\{\gamma_n\}$'s is shown in Fig. 1b together with the predictions of RMT for the circular unitary ensemble (CUE) [12]. In spite of the general good agreement, it deviates systematically from the numerical result (see inset), and it does not reproduce the sharp gap in the width spectrum. The cross section fluctuations depend crucially on $\langle\gamma\rangle_k$, which can be approximated by the classical decay constant $\langle\gamma\rangle_k = \gamma_{cl}$ (see Fig. 3b below). For the v regular graphs discussed above, $\gamma_{cl} \approx \frac{4}{2\pi}\frac{v}{1+v}\frac{V}{1+v}$. By changing v and V we can control the degree of overlap, allowing one to test various phenomena, as will be described below.

We use Eq. (8) to study the resonance correlation function in terms of its form factor,
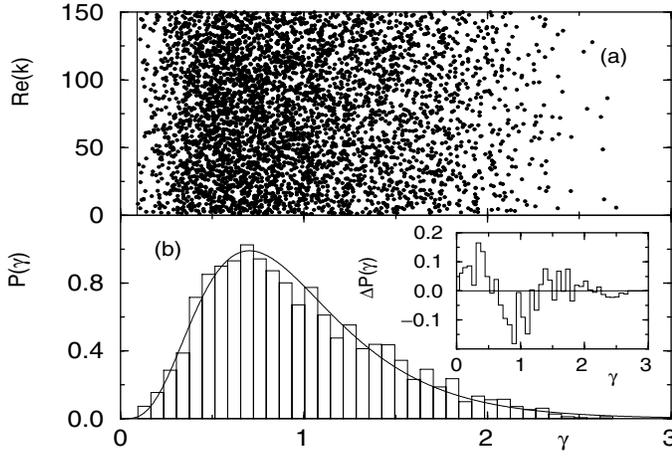
FIG. 1.   (a) The 5000 resonances of a single realization of a pentagon with $A \neq 0$. The solid line marks the position of the gap γ_{gap}. (b) The distribution $\mathcal{P}(\gamma)$. The solid line is the RMT prediction [12]. The difference $\mathcal{P}(\gamma) - \mathcal{P}_{\text{CUE}}(\gamma)$ is shown in the inset.

$$K_R(t) \equiv \int d\chi \, e^{i2\pi\chi\mathcal{L}t} \left\langle \tilde{d}_R\left(k + \frac{\chi}{2}\right) \tilde{d}_R\left(k - \frac{\chi}{2}\right) \right\rangle_k, \tag{10}$$

where $\tilde{d}_R(k)$ is the oscillatory part of $d_R(k)$. By substituting (8), we find that the value of $K_R(t)$ equals the squared sum of amplitudes $\tilde{\mathcal{A}}_p$ of the periodic orbits of length $rl_p = t\mathcal{L}$. A similar sum contributes to the spectral form factor of the *compact* graph $\mathcal{G}$ [1]. The corresponding amplitudes are different due to the fact that $\tilde{\mathcal{A}}_p$ also includes the information about the escape of flux to the leads. Assuming that all periodic orbits decay at the same rate, one would expect $K_R(t) \approx K(t)e^{-\gamma_{\text{cl}}t}$, where $K(t)$ is the form factor for the compact system [13]. This simple approximation is checked in the inset of Fig. 2 (see dashed line) and it is shown to reproduce the numerical data rather well in the domain $t \lesssim 5$. The asymptotic decay is dominated
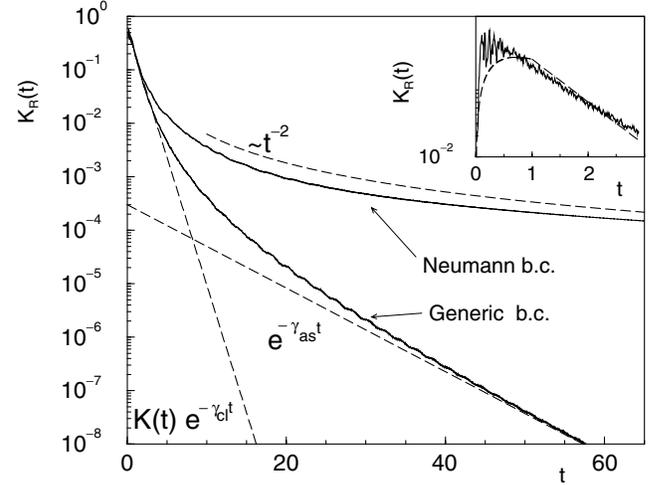
FIG. 2.   The form factor $K_R(t)$ for a pentagon with generic and Neumann boundary conditions with the same mean resonance width $\langle\gamma\rangle_k$ and $A \neq 0$. The data were averaged over 5000 spectral intervals and smoothed on small t intervals. In the inset we show $K_R(t)$ for small times. The solid line corresponds to the numerical data for the pentagon with generic boundary conditions, while the dashed line is the approximant $K_R(t) \approx K(t)\exp(-\gamma_{\text{cl}}t)$.

by the resonances which are nearest to the gap, and it cannot be captured by the crude argument presented above. For a generic graph, K_R decays exponentially but with a rate given by $\gamma_{\text{as}} = \gamma_{\text{gap}}$ (the best fit, indicated in Fig. 2 by the dashed line, gives γ_{as} which deviates by 30% from γ_{gap}). For the graph with Neumann boundary conditions, $\gamma_{\text{gap}} = 0$, and one expects an asymptotic power-law decay. (The corresponding dashed line in Fig. 2 shows t^{-2}.)

Another signature of overlapping resonances is the Ericson fluctuations observed in the k dependence of the scattering cross sections. They are one of the prominent features which characterizes generic chaotic scattering in the semiclassical limit. A convenient measure for Ericson fluctuations is the autocorrelation function

$$C(\chi; \nu) = \frac{1}{\Delta j} \sum_{j=j_{\min}}^{j_{\max}} \left\langle S_{j,j+\nu}^{(V)}\left(k + \frac{\chi}{2}\right) S_{j,j+\nu}^{(V)\star}\left(k - \frac{\chi}{2}\right) \right\rangle_k, \tag{11}$$

where $\Delta j = j_{\max} - j_{\min} + 1$. By substituting (5) in (11), we split the sum over trajectories into two distinct parts: the contributions of short trajectories are computed explicitly by following the multiple scattering expansion up to trajectories of length $l_{\max}$. The contribution of longer orbits is approximated by using the diagonal approximation, which results in a Lorentzian with a width γ_{Er}, expected to be well approximated by γ_{cl}. Including explicitly up to $n = 3$ scatterings, we get

$$C(\chi; \nu) \approx G e^{il_{\max}\chi} \frac{\gamma_{\text{Er}}}{\gamma_{\text{Er}} - i\chi} + \frac{1}{\Delta j} \sum_{j=j_{\min}}^{j_{\max}} \left[\tau^4 e^{i\chi L_{j,j+\nu}} + \tau^4 \rho^4 e^{3i\chi L_{j,j+\nu}} + \tau^6 \sum_{m \neq j, j+\nu} e^{i\chi(L_{j,m} + L_{m,j+\nu})} \right], \tag{12}$$

where the constant G is determined by the normalization condition $C(\chi = 0; \nu) = 1$. The interplay between the contributions of long and short periodic orbits is shown in Fig. 3a. For overlapping resonances, the autocorrelation function is well reproduced by the Lorentzian expected from the standard theory of Ericson fluctuations. The other case corresponds to isolated resonances, where the con-

tributions of short paths are clearly seen. From each of the various statistical measures of the resonance density and the cross section fluctuations discussed above, we extracted the effective average γ, which would best fit the numerical data. In Fig. 3b we compare these numerical values, with the classical expectation, and the predictions
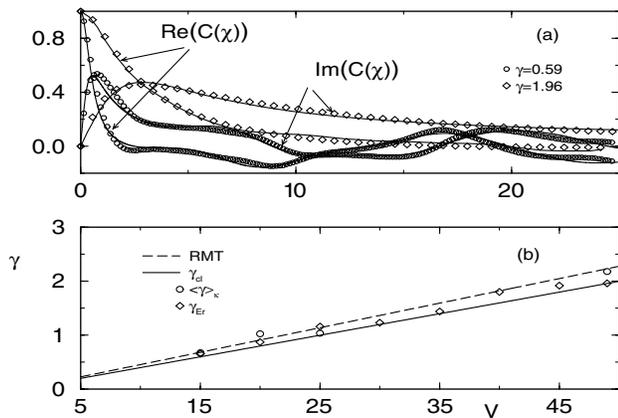
FIG. 3. Regular graphs with "Neumann" boundary conditions: (a) The real and the imaginary part of $C(\chi, \nu = 1)$ for isolated ($\circ$) and overlapping ($\diamond$) resonances. The solid lines correspond to the theoretical expression (12). (b) The mean resonance width $\langle\gamma\rangle_k$, autocorrelation width γ_{Er}, the classical expectation γ_{cl}, and the RMT prediction [12] vs V for constant valency $\nu = 14$.

of RMT [12]. The results justify the use of the classical estimate for the computation of these quantities, especially in the limit $V \rightarrow \infty$ for fixed ν/V (which is the analog of the semiclassical limit). In this limit, the RMT and the classical estimate coincide.

To investigate further the statistical properties of the $S^{(V)}$ matrix, we study the distribution of scaled partial Wigner delay times $T = \frac{\Delta}{2\pi}\frac{\partial\theta_r(k)}{\partial k}$. The resulting distribu-
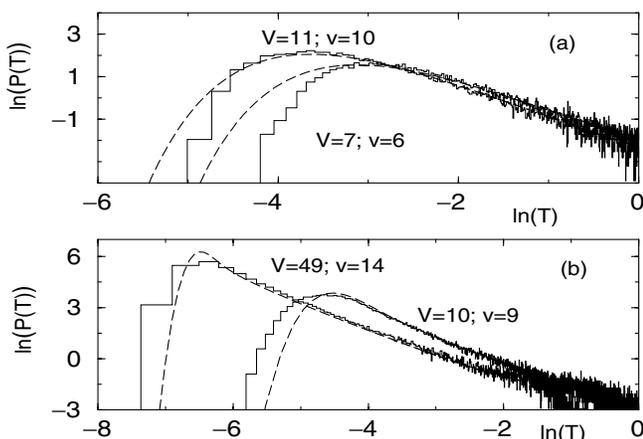
FIG. 4. The distribution of the scaled partial delay times T for various graphs with Neumann boundary conditions. The dashed lines correspond to the RMT expectation [12]. (a) One channel and $A = 0$; (b) V channels and $A \neq 0$.

tion for various graphs with $A = 0$ and $A \neq 0$ are shown in Figs. 4a and 4b, respectively, together with the predictions of RMT [12]. An overall agreement is evident. Deviations appear at the short time regime (i.e., short orbits), during which the chaotic component due to multiple scattering is not yet fully developed [14].

In summary, we presented analytical and numerical results, on the basis of which we propose quantum graphs as a model for the study of quantum chaotic scattering. Their simplicity enables us to obtain a new understanding of the subject. Because of lack of space, we defer the discussion of other results and further comparisons with RMT to a later publication [15].

[1] Tsampikos Kottos and Uzy Smilansky, Phys. Rev. Lett. **79**, 4794 (1997); Ann. Phys. (N.Y.) **273**, 1 (1999).

[2] U. Smilansky, in *Les Houches Summer School on Chaos and Quantum Physics,* edited by M.-J. Giannoni *et al.* (North-Holland, Amsterdam, 1989), pp. 371–441.

[3] P. Gaspard, in *Proceedings of E. Fermi Summer School 1991,* edited by G. Casati *et al.* (North-Holland, Amsterdam, 1993), p. 307.

[4] I. Rotter, Rep. Prog. Phys. **54**, 635 (1991).

[5] *Atomic Spectra and Collisions in External Fields,* edited by M. H. Nayfeh *et al.* (Plenum, New York, 1989), Vol. 2.

[6] D. Stone in *Proceedings of the 1994 Les Houches Summer School on Mesoscopic Quantum Physics,* edited by E. Akkermans *et al.* (North-Holland, Amsterdam, 1995), pp. 373–433.

[7] E. Doron, U. Smilansky, and A. Frenkel, Phys. Rev. Lett. **65**, 3072 (1990); H. J. Stöckmann and J. Stein, Phys. Rev. Lett. **64**, 2215 (1990).

[8] P. Gaspard and S. A. Rice, J. Chem Phys **90**, 2225 (1989); **90**, 2242 (1989); **90**, 2255 (1989); **91**, E3279 (1989).

[9] W. H. Miller, Adv. Chem. Phys. **25**, 69 (1974).

[10] C. Mahaux and H. A. Weidenmuller, *Shell Model Approach in Nuclear Reactions* (North-Holland, Amsterdam, 1969).

[11] M. Sh. Birman and D. R. Yafaev, St. Petersburg Math. J. **4**, 833 (1993).

[12] Y. Fyodorov and H-J Sommers, J. Math. Phys. **38**, 1918 (1997).

[13] B. Eckhardt, I. Varga, and P. Pollner (to be published).

[14] R. Blümel and U. Smilansky, Phys. Rev. Lett. **64**, 241 (1990).

[15] Tsampikos Kottos and Uzy Smilansky (to be published).